Solid Solutions in Metal Complexes. Solubility Phase Diagrams and X-Ray Crystal Structures of *trans*(*N*,*t*-*N*)-[Co(norleucinato)(tren)]I_2 and *trans*(*N*,*t*-*N*)-[Co(methioninato)(tren)]I_2 [tren=tris(2-aminoethyl)amine]

Kazuaki Yamanari* **and Akira Fuyuhiro**

Department of Chemistry, Faculty of Science, Osaka University, Toyonaka, Osaka 560

(Received February 20, 1995)

Ternary solubility diagrams of *trans*(*N*,*t*-*N*)-[Co(n-leu)(tren)]I_2 and *trans*(*N*,*t*-*N*)-[Co(met)(tren)]I_2 [*t*-*N*=tertiary amine nitrogen, n-leu=norleucinate(1-), met=methioninate(1-), and tren=tris(2-aminoethyl)-amine] were determined at 25.0 °C. A single isotherm was found; the tie lines do not converge to any apexes of the enantiomers in either system. The solid phases are variable over the entire region from D : L(%)=100 : 0 to 0 : 100, and both systems form a solid solution. The X-ray crystal structures of *trans*(*N*,*t*-*N*)-[Co(DL-n-leu)(tren)]I_2 (**1**; D : L=50 : 50) and *trans*(*N*,*t*-*N*)-[Co(DL-met)(tren)]I_2 (**3**; D : L=50 : 50) were determined from 3600 and 4699 reflections to R=0.036 (R_w=0.046) and R=0.045 (R_w=0.068), respectively: space group $P2_1/c$ with a=9.204(4), b=11.057(2), c=19.576(3) Å, β=95.95(2)°, and Z=4 for **1** and space group $P2_1/n$ with a=13.032(4), b=11.210(4), c=13.535(2) Å, β=92.62(2)°, and Z=4 for **3**. The results confirm the co-existence of the D- and L-amino acidato complex ions in each site of the unit cell in both complexes. Furthermore, the unit cell comprises two D-rich sites and two L-rich sites: The unequal occupancy of the D- and L-amino acidato complex ions in each site is found irrespective of the racemic composition.

Crystalline racemates belong to one of three different classes: a racemic compound, a conglomerate, and a solid solution. The latter two cases have so far been very limited.[1] Recently, we have communicated the first examples of racemic solid solutions containing amino acidate in [Co(leu)$(NH_3)_4$]Br_2 and [Co(leu)$(NH_3)_4$]I_2 [leu=leucinate (1-)][2] and conglomeratic solid solutions in *trans*(*N*,*t*-*N*)-[Co(leu)(tren)]I_2 and *trans*(*N*,*t*-*N*)-[Co(n-leu)(tren)]$[ClO_4]_2$ [n-leu=norleucinate(1-) and tren=tris(2-aminoethyl)amine].[3] In the former racemic solid solution one flat isotherm was observed at 25.0 °C over the entire range of concentrations; in the latter there are two branches of the solubility curve and one invariant point at 25.0 °C. In both systems the tie lines do not converge to any apexes of the enantiomers, but diverse widely, which is a typical characteristic of a solid solution. The existence of such solid solutions have been firmly identified by X-ray crystal analyses.

These findings suggest the frequent occurrence of rare solid solutions in amino acidato metal complexes, which has prompted us to carry out additional investigations of the solubility phase diagrams and X-ray crystal analyses of other amino acidato complexes. In this paper we describe new solid solutions in *trans*(*N*,*t*-*N*)-[Co(n-leu)(tren)]I_2 and *trans*(*N*,*t*-*N*)-[Co(met)(tren)]I_2 [met=methioninate(1-)].

Experimental

Preparations of *trans*(*N*,*t*-*N*)-[Co(DL-n-leu)(tren)]I_2 (**1**), *trans*(*N*,*t*-*N*)-[Co(L-n-leu)(tren)]I_2 (**2**), *trans*(*N*,*t*-*N*)-[Co(DL-met)(tren)]I_2 (**3**), and *trans*(*N*,*t*-*N*)-[Co(L-met)(tren)]I_2 (**4**). These complexes were prepared from [Co$(Cl)_2$(tren)]-Cl and an equimolar of amino acid and KOH according to a method by Akamatsu et al.[4] The desired iodide of the DL- or L-n-leu complex was obtained by adding a calculated amount of KI to the resultant chloride solution. In the DL- or L-met system, a double salt [Co(DL- or L-met)(tren)]ICl was obtained instead of the iodide. The salt was converted to pure iodide using a column of QAE-Sephadex A-25 (I^- form). All of the complexes were recrystallized from water. The yields were ca. 70—80%.

Complex **1** {Found: C, 24.53; H, 5.20; N, 11.85%. Calcd for *trans*(*N*,*t*-*N*)-[Co(DL-n-leu)(tren)]I_2, $C_{12}H_{30}N_5O_2CoI_2$: C, 24.46; H, 5.13; N, 11.89%}: VIS (water) λ_{max}/nm 471 (ε/dm^3 mol^{-1} cm^{-1} 124.3) and 342 (118).

Complex **2** {Found: C, 24.61; H, 5.25; N, 11.92%. Calcd for *trans*(*N*,*t*-*N*)-[Co(L-n-leu)(tren)]I_2, $C_{12}H_{30}N_5O_2CoI_2$: C, 24.46; H, 5.13; N, 11.89%}: VIS (water) λ_{max}/nm 471 (ε/dm^3 mol^{-1} cm^{-1} 124.3) and 342 (116): CD (water) λ_{ext}/nm 510 ($\Delta\varepsilon$/dm^3 mol^{-1}cm^{-1} +0.185), 455 (−0.820), and 343 (+0.140).

Complex **3** {Found: C, 21.76; H, 4.68; N, 11.49%. Calcd for *trans*(*N*,*t*-*N*)-[Co(DL-met)(tren)]I_2, $C_{11}H_{28}N_5SO_2CoI_2$: C, 21.76; H, 4.65; N, 11.53%}: VIS (water) λ_{max}/nm 472

(ε/dm^3 mol^{-1} cm^{-1} 125.0) and 338 (138).

Complex **4** {Found: C, 21.86; H, 4.55; N, 11.48%. Calcd for *trans*(*N*,*t*-*N*)-[Co(L-met)(tren)]I_2, $C_{11}H_{28}N_5SO_2CoI_2$: C, 21.76; H, 4.65; N, 11.53%}: VIS (water) λ_{max}/nm 472 (ε/dm^3 mol^{-1} cm^{-1} 124.7) and 338 (137): CD (water) λ_{ext}/nm 509 ($\Delta\varepsilon$/dm^3 mol^{-1} cm^{-1} +0.263), 454 (−0.769), and 340 (+0.121).

Solubility Measurements. The solubilities of complexes in water were determined according to the same procedure as previously reported.[2] The binary solubilities are collected in Table 1. In the ternary isotherm, the measurement of one point needed stirring for ca. 24 h, because the establishment of a true solubility equilibrium would require a continuous change in the composition of the solid phase concomitantly with that of the solution. The composition of the equilibrated solution was determined on the basis of the absorption and circular dichroism (CD) spectral measurements. The composition of the solid in equilibrium with the solution was determined in the same way as described above using a solid sample free from the mother liquor. The solid phases were also identified by elemental analysis and infrared (IR) spectra.

Table 1. Binary Solubilities of *trans*(*N*,*t*-*N*)-[Co(am)-(tren)]I_2 **1**—**4**[a]

	Complex		Solubility	Complex		Solibility
	1	**2**	ratio	**3**	**4**	ratio
T/°C	am=DL-n-leu	L-n-leu	DL/L	DL-met	L-met	DL/L
5.0	0.99	1.75	0.57	0.96	1.68	0.57
10.0	1.14	2.08	0.55	1.16	2.05[b]	0.57
15.0	1.38	2.36	0.58	1.41	2.45	0.58
20.0	1.55	2.70	0.57	1.69	2.93	0.58
25.0	1.88	3.17	0.59	2.01	3.51	0.57
30.0	2.07	3.61	0.57	2.43	4.21	0.58
35.0	2.47	4.17	0.59	2.91	5.07	0.57
40.0	2.76	4.76	0.58	3.49	6.03	0.58
45.0	3.25	5.51	0.59	4.13	7.57	0.55
50.0	3.74	6.32	0.59			
55.1	4.39	7.43	0.59			

a) Grams of anhydrous salt in 100 g of water. b) Value at 10.1 °C.

X-Ray Crystallography. Single crystals of complexes **1** and **3** were obtained from their racemic aqueous solutions, respectively, and were mounted on glass fibers with epoxy cement. The data were collected on a Rigaku AFC5R diffractometer using graphite monochromated Mo$K\alpha$ radiation (λ=0.71069 Å) and solved by TEXSAN.[5] Block diagonal matrix least-squares refinements were used. Decay and absorption corrections were applied, and redundant data were removed. The crystal data are given in Table 2. There were disordered parts in both structures, which were asymmetric carbons C(8) and the side chains of amino acids; however, the three terminal atoms of the side chains were solved as an accidental overlap. The C(8) and C(9) atoms were firstly solved as two sites with equal occupancy (0.5), respectively. Then, the occupancy A : B was varied and the minimum R value was searched, providing A : B=83 : 17 for complex **1** and A : B=77 : 23 for complex **3**. All of the non-hydrogen atoms were refined anisotropically, except for the A and B carbons; hydrogen atoms were included in calculated positions.

Measurements. The absorbances were measured using a Hitachi 330 spectrophotometer, CD spectra with a JASCO J-500 spectropolarimeter, and IR spectra with a Shimadzu IR-435 spectrophotometer. The X-ray crystal analyses were carried out at the X-ray Diffraction Service of the Department of Chemistry.

Results and Discussion

Preparation and Characterization of Com-

Table 2. Crystal Data for *rac*-*trans*(*N*,*t*-*N*)-[Co(n-leu)(tren)]I_2 (**1**) and *trans*(*N*,*t*-*N*)-[Co(DL-met)(tren)]I_2 (**3**)

	1	**3**
Formula	$C_{12}H_{30}O_2N_5CoI_2$	$C_{11}H_{28}O_2N_5SCoI_2$
Fw	589.14	607.18
Space group	$P2_1/c$ (No. 14)	$P2_1/n$ (No. 14)
Crystal dimension/mm	0.20×0.15×0.30	0.30×0.30×0.25
a/Å	9.204(4)	13.032(4)
b/Å	11.057(2)	11.210(4)
c/Å	19.576(3)	13.535(2)
β/deg	95.95(2)	92.62(2)
V/Å^3	1981(2)	1975.2(8)
Z	4	4
D_{calc}/g cm^{-1}	1.975	2.042
2θ range/deg	3—60	3—60
Temp/°C	23	23
h,k,l	+12,+16,±28	+18,+16,±19
No. of variables	221	221
No. of $I>3\sigma(I)$	3600	4699
R[a]	0.036	0.045
R_w[b]	0.046	0.068

a) $R=\sum||F_o|-|F_c||/\sum|F_o|$. b) $R_w=[(\sum w(|F_o|-|F_c|)^2/\sum w|F_o|^2)]^{1/2}$; $w=1/\sigma^2(F_o)$.

plexes. In the [Co(amino acidato-*N*,*O*)(tren)]X_2-type complex, there are two geometrical isomers, which are denoted as *cis*(*N*,*t*-*N*) and *trans*(*N*,*t*-*N*), concerning the mutual disposition between the NH_2 group of an amino acidate and the tertiary amine of tren (Fig. 1). In the present n-leu and met systems, only one geometrical isomer was obtained. Figure 2 shows the absorption and CD spectra of [Co(L-n-leu)(tren)]I_2 (**2**). Complex **2** (orange) exhibits the first d–d band at 471 nm and two CD components [(+) and (−)] from the lower energy side, in the same region. The absorption maximum and CD pattern are the same as those in *trans*(*N*,*t*-*N*)-[Co(L-val)(tren)]$^{2+}$ [orange isomer; L-val = L-valinate-(1-)].[4,6] The methioninato complexes, **3** (DL-met) and **4** (L-met), also show similar absorption spectra to that of *trans*(*N*,*t*-*N*)-[Co(L-val)(tren)]$^{2+}$. Hence, complexes **1**—**4** are assigned to the *trans*(*N*,*t*-*N*) isomer.

Two isomers, orange and red, have so far been prepared in [Co(glycinato)(tren)]$^{2+}$[6] and [Co(L-alaninato)(tren)]$^{2+}$.[4] However, it is well known that the formation of the red *cis*(*N*,*t*-*N*) isomer decreases along with an increase in the bulkiness of a substituent on the amino carboxylate ring, and only the orange isomer has been reported for each tren complex with L-valinate, L-serinate, L-phenylalaninate, and D-phenylglycinate.[4] The same phenomena were observed in the present norleucinate and methioninate systems.

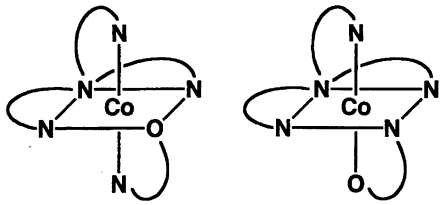

Fig. 1. Two geometrical isomers of [Co(amino acidato-*N*,*O*)(tren)]$^{2+}$.

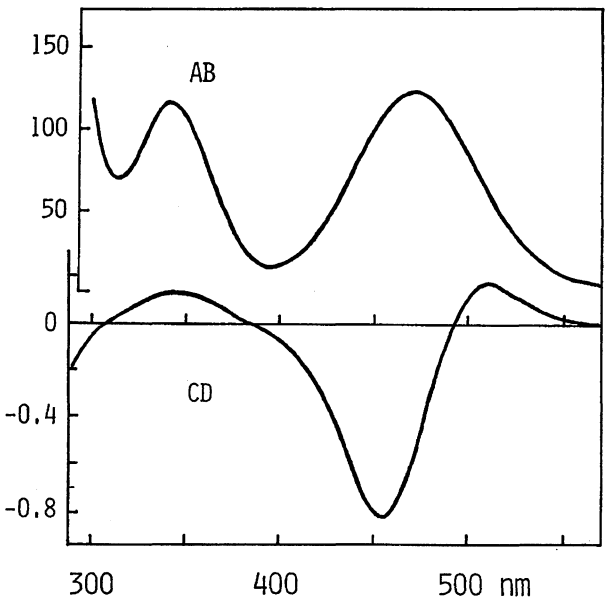

Fig. 2. Absorption and CD spectra of *trans*(*N*,*t*-*N*)-[Co(L-n-leu)(tren)]I_2 (**2**).

Solubility Phase Diagrams. Table 1 shows the binary solubilities of *trans*(*N*,*t*-*N*)-[Co(DL-n-leu)(tren)]-I_2 (**1**) and *trans*(*N*,*t*-*N*)-[Co(L-n-leu)(tren)]I_2 (**2**) at 5—55 °C. The solubility ratio (S_{DL}/S_L) is 0.57—0.59 in the region, and the racemate is less soluble than the enantiomer. The binary result apparently means that the racemate does not exist as a conglomerate but exists as a racemic compound.[7] In general, since a racemic compound has a different crystal structure from its enantiomer, their IR spectra must be different from each other. The racemate anhydrate and the enantiomer anhydrate, however, showed the same IR spectra. These facts mean that both complexes **1** and **2** are isomorphous, and belong to the same crystal structure, thus suggesting the formation of a solid solution at 5—55 °C.

To confirm the above-mentioned expectation, the ternary solubility isotherm of *trans*(*N*,*t*-*N*)-[Co(n-leu)-(tren)]I_2 was measured at 25 °C. As shown in Fig. 3, there is no eutectic point in this system, and the solubility curve starting from the racemic side overlaps with the curve starting from the enantiomeric side to give only one isotherm. The part of the phase diagram lying below the solubility curve constitutes a single region in which the tie lines diverge widely, and do not converge to any of the apexes of the racemate or the pure enantiomers. The results indicate that the iodide forms a single solid solution over the entire range of the D : L composition. Therefore, all solids gave the same IR spectra, irrespective of the differences in their compositions.

In the system of *trans*(*N*,*t*-*N*)-[Co(met)(tren)]I_2

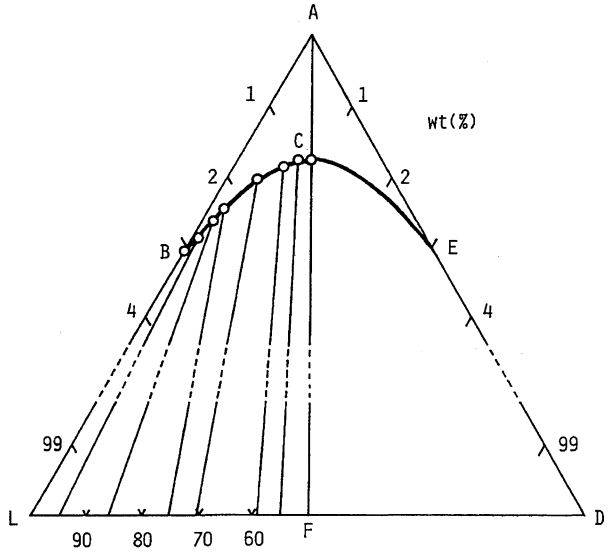

Fig. 3. Ternary solubility isotherm of the system, H_2O(A)---*trans*(*N*,*t*-*N*)-[Co(L-n-leu)(tren)]I_2(L)---*trans*(*N*,*t*-*N*)-[Co(D-n-leu)(tren)]I_2(D), at 25 °C.

(Table 2 and Fig. 4), the racemate is less soluble than the enantiomer: the solubility ratio (S_{DL}/S_L) is 0.55—0.57 at 5—45 °C. This indicates that the racemate is thermodynamically more stable than the enantiomer, and exists as a racemic compound.[7] However, both the racemate anhydrate and the enantiomer anhydrate showed the same IR spectra. In the ternary isotherm at 25 °C, the single isotherm, no eutectic point, and divergence of the tie lines, which are typical characteristics of a solid solution, can all be seen. Thus, this system also forms a solid solution: The solid phases are variable over the entire region from D : L(%)=100 : 0 to 0 : 100.

The present ternary isotherms are slightly different from those of $[Co(leu)(NH_3)_4]X_2$ (X=Br and I).[2] The latter isotherms are flat and close to an ideal solid solution, because the solubilities of the racemate and the enantiomer are almost equal [the solubility ratio (S_{DL}/S_L) is 0.95 for bromide and 0.97 for iodide at 25 °C]. Since the relative stabilities of the racemate and the enantiomer are equal in an ideal solid solution, the D- and L-molecules are freely exchangeable without any free-energy loss at any composition. On the other hand, the present isotherm swells in the center part, because the racemate is less soluble than the enantiomer. This means that the racemate is more stable than the enantiomer. Accordingly, the crystal-packing modes in the racemate and in the enantiomer of the present systems are expected to be different from those in a pseudo-ideal solid solution.

Molecular Structures. The crystal data are summarized in Table 2. The number of non-hydrogen atoms is equal in complexes **1** and **3**, and C(11) of **1** corresponds to S of **3** and C(12) of **1** to C(11) of **3**. The numberings of the other atoms are the same, except for I(1) and I(2). The atomic coordinates of non-hydrogen atoms are given in Table 3 (complex **1**) and Table 4 (complex **3**). The selected bond distances and the bond angles of both complexes are given in Tables 5 and 6, respectively.

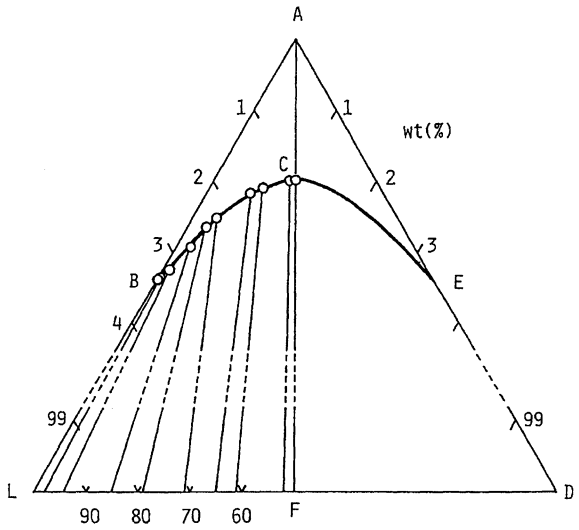

Fig. 4. Ternary solubility isotherm of the system, H_2O(A)---*trans*(*N*,*t*-*N*)-[Co(L-met)(tren)]I_2(L) ---*trans*(*N*,*t*-*N*)-[Co(D-met)(tren)]I_2(D), at 25 °C.

Figure 5 shows an ORTEP[8] drawing of the cation of *trans*(*N*,*t*-*N*)-[Co(DL-n-leu)(tren)]I_2 (**1**). Though two geometrical isomers are possible in the [Co(amino acidato-*N*,*O*)(tren)]$^{2+}$, complex **1** adopts the *trans*(*N*, *t*-*N*) structure, as expected from the absorption spectrum. This crystal has the racemic composition with D : L=50 : 50, but is not a racemic compound. The A-[C(8A) and C(9A)] and B-atoms [C(8B) and C(9B)] denote a part of the D- and L-norleucinates, respectively. It has been clearly demonstrated that the D- and L-norleucinato complex ions occupy the same site in the unit cell, which firmly indicates the existence of a solid solution. Furthermore, the site occupancies of the A- and B-atoms are not even. The D-norleucinate is rich in this site: the occupancy ratio is A : B(%)=83 : 17.

The structure of the ordered part is close to that of *trans*(*N*,*t*-*N*)-[Co(gly)(tren)]Cl[ClO_4] (gly = glycinate):[6] The bond distances are all within 0.02 Å and the bond angles are within 2°. On the other hand, the bond distances and angles concerning C(8), C(9), C(10), C(11), and C(12) in Tables 5 and 6 are not normal, because there is a disorder for these five atoms, and the terminal three atoms cannot be separated into two chains, and are solved as accidental overlaps.

Table 3. Positional and Isotropic-Equivalent Thermal Displacement Parameters (B_{eq} in Å^2)[b] for **1**

Atom	*x*	*y*	*z*	B_{eq}
I(1)	0.31489(5)	0.03525(4)	0.09503(2)	3.80(2)
I(2)	0.73463(5)	0.13781(4)	0.24785(3)	3.99(2)
Co	0.38438(7)	0.22930(6)	0.37731(3)	2.00(3)
O(1)	0.3335(4)	0.1433(3)	0.4557(2)	2.4(1)
O(2)	0.4206(4)	0.0763(4)	0.5585(2)	3.1(2)
N(1)	0.1885(5)	0.2179(4)	0.3303(2)	2.5(2)
N(2)	0.3172(5)	0.3786(4)	0.4182(2)	2.7(2)
N(3)	0.4371(5)	0.3177(4)	0.2973(2)	2.6(2)
N(4)	0.4196(5)	0.0718(4)	0.3364(2)	2.6(2)
N(5)	0.5807(5)	0.2322(4)	0.4259(2)	2.6(2)
C(1)	0.0894(6)	0.2812(6)	0.3750(3)	3.1(2)
C(2)	0.1593(7)	0.3997(6)	0.3972(3)	3.5(3)
C(3)	0.1829(7)	0.2774(6)	0.2605(3)	3.3(2)
C(4)	0.3330(7)	0.2882(5)	0.2375(3)	3.1(2)
C(5)	0.1557(6)	0.0851(5)	0.3252(3)	3.2(2)
C(6)	0.2840(7)	0.0233(5)	0.2977(3)	3.2(2)
C(7)	0.4340(6)	0.1358(5)	0.5072(3)	2.6(2)
C(8A)[a]	0.5643(8)	0.2199(6)	0.5021(4)	2.7(1)
C(8B)[a]	0.590(3)	0.182(3)	0.495(2)	2.0(5)
C(9A)[a]	0.7047(8)	0.1724(6)	0.5424(4)	3.1(1)
C(9B)[a]	0.663(5)	0.247(4)	0.546(2)	5(1)
C(10)	0.8294(7)	0.2667(6)	0.5432(4)	4.7(3)
C(11)	0.960(1)	0.222(1)	0.5922(5)	6.9(5)
C(12)	1.049(1)	0.125(1)	0.5666(5)	7.6(6)

a) The populations are 0.83 for C(8A) and C(9A), and 0.17 for C(8B) and C(9B).

b) $B_{eq}=(8\pi^2/3)\sum_{i=1}^{3}\sum_{j=1}^{3} U_{i,j}\, a_i^* a_j^* \boldsymbol{a}_i \cdot \boldsymbol{a}_j$.

Table 4. Positional and Isotropic-Equivalent Thermal Displacement Parameters (B_{eq} in Å^2)[b] for **3**

Atom	x	y	z	B_{eq}
I(1)	0.48158(3)	0.52329(4)	0.18487(3)	3.74(2)
I(2)	0.13119(4)	0.62777(4)	0.13124(3)	4.04(2)
Co	0.31655(5)	0.21988(6)	0.05672(5)	1.95(2)
S	0.8085(2)	0.2016(2)	0.1630(1)	4.45(8)
O(1)	0.3745(2)	0.1344(3)	−0.0490(3)	2.3(1)
O(2)	0.5211(3)	0.0684(4)	−0.1053(3)	3.3(2)
N(1)	0.1779(3)	0.2119(4)	−0.0013(3)	2.5(2)
N(2)	0.3320(4)	0.3675(4)	−0.0190(3)	2.8(2)
N(3)	0.2597(3)	0.3072(4)	0.1655(3)	2.7(2)
N(4)	0.2865(3)	0.0636(4)	0.1157(3)	2.5(2)
N(5)	0.4571(3)	0.2218(4)	0.1130(3)	2.5(2)
C(1)	0.1791(4)	0.2796(6)	−0.0968(4)	3.2(2)
C(2)	0.2345(5)	0.3934(6)	−0.0780(4)	3.4(2)
C(3)	0.1016(4)	0.2685(6)	0.0671(4)	3.3(2)
C(4)	0.1494(4)	0.2773(5)	0.1713(4)	3.0(2)
C(5)	0.1557(4)	0.0832(5)	−0.0179(4)	3.1(2)
C(6)	0.1850(4)	0.0178(5)	0.0766(5)	3.3(2)
C(7)	0.4736(4)	0.1271(5)	−0.0467(4)	2.4(2)
C(8A)[a]	0.5253(5)	0.2116(6)	0.0285(5)	2.5(1)
C(8B)[a]	0.538(2)	0.167(2)	0.050(2)	2.0(3)
C(9A)[a]	0.6324(6)	0.1689(7)	0.0620(6)	3.1(1)
C(9B)[a]	0.611(2)	0.252(2)	0.010(2)	2.9(4)
C(10)	0.6955(5)	0.2756(7)	0.1087(5)	4.5(3)
C(11)	0.8789(5)	0.3310(8)	0.2015(6)	4.6(3)

a) The populations are 0.77 for C(8A) and C(9A), and 0.23 for C(8B) and C(9B).

b) $B_{eq}=(8\pi^2/3)\sum_{i=1}^{3}\sum_{j=1}^{3} U_{i,j}a_i^* a_j^* \boldsymbol{a}_i\cdot\boldsymbol{a}_j$.

Table 5. Selected Bond Distances (Å)

	1	**3**
Co–O(1)	1.905(4)	1.906(4)
Co–N(1)	1.942(4)	1.939(4)
Co–N(2)	1.963(5)	1.962(5)
Co–N(3)	1.949(5)	1.943(5)
Co–N(4)	1.958(5)	1.972(5)
Co–N(5)	1.953(4)	1.952(4)
O(1)–C(7)	1.298(6)	1.293(6)
O(2)–C(7)	1.219(7)	1.221(7)
N(1)–C(1)	1.501(8)	1.499(7)
N(1)–C(3)	1.513(7)	1.527(7)
N(1)–C(5)	1.500(7)	1.486(8)
N(2)–C(2)	1.488(8)	1.499(8)
N(3)–C(4)	1.470(7)	1.481(7)
N(4)–C(6)	1.491(8)	1.493(7)
N(5)–C(8A)	1.520(8)	1.485(8)
N(5)–C(8B)	1.45(3)	1.52(2)
C(1)–C(2)	1.504(9)	1.482(9)
C(3)–C(4)	1.50(1)	1.519(8)
C(5)–C(6)	1.511(9)	1.508(9)
C(7)–C(8A)	1.529(9)	1.526(8)
C(7)–C(8B)	1.57(3)	1.59(2)
C(8A)–C(9A)	1.54(1)	1.52(1)
C(8B)–C(9B)	1.36(5)	1.46(3)
C(9A)–C(10)	1.55(1)	1.57(1)
C(9B)–C(10)	1.56(5)	1.72(2)
C(10)–C(11)	1.54(1)	—
C(10)–S	—	1.817(7)
C(11)–C(12)	1.47(1)	—
S–C(11)	—	1.781(8)

Figure 6 shows an ORTEP drawing of *trans*(*N*,*t*-*N*)-[Co(DL-met)(tren)]I_2 (**3**). This racemic complex also forms a solid solution. The A- [C(8A) and C(9A)] and B-atoms [C(8B) and C(9B)] denote the L- and D-methioninates, respectively. Both the L- and D-methioninate ions exist together in each site of the crystal unit. The unequal occupancy was confirmed in this complex. The L-methioninate is rich in the present site and the occupancy ratio is A : B(%)=77 : 23. It should be, of course, noted that the entire crystal has the racemic composition. The bond distances and angles of the ordered part are close to those of *trans*(*N*,*t*-*N*)-[Co(gly)(tren)]-Cl[ClO_4].[6] However, the values for C(8), C(9), C(10), S, and C(11) in Tables 5 and 6 are not normal because of the disorder of these five atoms.

Comparison of Molecualr Structures. The bond distances and angles for the orderd parts of *trans*(*N*,*t*-*N*)-[Co(DL-n-leu)(tren)]I_2 (**1**) and *trans*(*N*, *t*-*N*)-[Co(DL-met)(tren)]I_2 (**3**) are very similar to each other (Tables 5 and 6). Table 7 lists the selected torsion angles of both complexes. Since the absolute configuration of the amino acidate in the major A-site is reverse between complexes **1** and **3**, the signs of the corresponding values become opposite, though the absolute values are similar to each other. The most striking difference is in the end part of the side chain. The torsion angle, C(9A)–C(10)–C(11)–C(12), is 76(1)° in complex **1**,

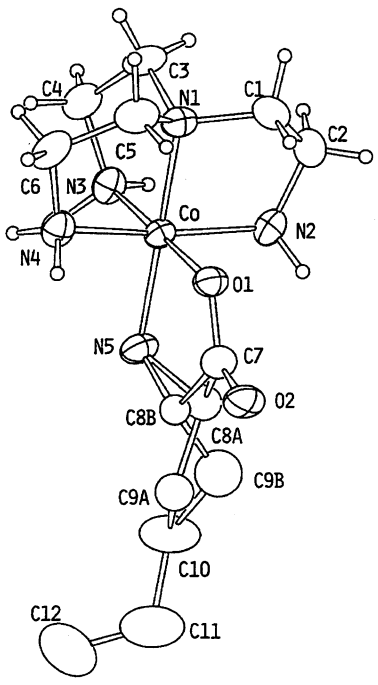

Fig. 5. An ORTEP drawing of *trans*(*N*,*t*-*N*)-[Co(DL-n-leu)(tren)]$^{2+}$ (**1**) with thermal ellipsoids drawn at the 50% probability level.

Table 6. Selected Bond Angles (deg)

	1	3
O(1)–Co–N(5)	84.7(2)	84.3(2)
N(1)–Co–N(2)	86.1(2)	86.8(2)
N(1)–Co–N(3)	87.0(2)	87.1(2)
N(1)–Co–N(4)	86.2(2)	85.6(2)
Co–O(1)–C(7)	116.3(3)	116.4(3)
Co–N(1)–C(1)	106.5(3)	106.2(3)
Co–N(1)–C(3)	110.1(3)	110.8(3)
Co–N(1)–C(5)	105.4(3)	106.1(3)
C(1)–N(1)–C(3)	111.0(4)	110.1(4)
C(1)–N(1)–C(5)	111.4(4)	111.7(4)
C(3)–N(1)–C(5)	112.2(4)	111.6(4)
Co–N(2)–C(2)	111.0(3)	109.7(4)
Co–N(3)–C(4)	109.4(4)	109.3(3)
Co–N(4)–C(6)	111.3(3)	110.6(3)
Co–N(5)–C(8A)	107.2(4)	106.4(3)
Co–N(5)–C(8B)	114(1)	116.2(8)
N(1)–C(1)–C(2)	107.9(5)	108.2(4)
N(2)–C(2)–C(1)	108.7(5)	108.6(5)
N(1)–C(3)–C(4)	111.0(5)	109.8(4)
N(3)–C(4)–C(3)	108.9(5)	108.9(5)
N(1)–C(5)–C(6)	107.9(5)	107.7(5)
N(4)–C(6)–C(5)	107.4(4)	108.6(5)
O(1)–C(7)–O(2)	123.4(5)	123.7(5)
O(1)–C(7)–C(8A)	114.2(5)	112.8(5)
O(1)–C(7)–C(8B)	116(1)	119.5(9)
O(2)–C(7)–C(8A)	122.0(5)	123.1(5)
O(2)–C(7)–C(8B)	119(1)	115.0(8)
N(5)–C(8A)–C(7)	106.1(5)	107.5(5)
N(5)–C(8A)–C(9A)	111.8(6)	111.6(5)
C(7)–C(8A)–C(9A)	112.5(6)	111.9(5)
N(5)–C(8B)–C(7)	108(2)	103(1)
N(5)–C(8B)–C(9B)	118(3)	115(2)
C(7)–C(8B)–C(9B)	116(3)	102(2)
C(8A)–C(9A)–C(10)	111.0(6)	109.6(6)
C(8B)–C(9B)–C(10)	117(4)	102(2)
C(9A)–C(10)–C(11)	108.7(6)	—
C(9A)–C(10)–S	—	102.5(5)
C(9B)–C(10)–C(11)	130(2)	—
C(9B)–C(10)–S	—	137(1)
C(10)–C(11)–C(12)	111.6(8)	—
C(10)–S–C(11)	—	98.3(3)

whereas the corresponding angle, C(9A)–C(10)–S–C(11), is 174.2(5)° in complex **3**. Although complex **1** adopts a *gauche* conformation, complex **3** is a *trans* one.

Crystal Structures. There exists a head-to-head contact between a cation and an ajacent cation in both crystals. Figure 7 shows stereoviews of the contacts, which are quite similar to each other in complexes **1** and **3**. The contact occurs due to a pair of hydrogen bonds between N(4) and O(2). The distance is 2.906(6) Å in complex **1** and 2.921(6) Å in complex **3**. The dotted molecules in complexes **1** and **3** of Fig. 7 denote the dominant L-amino acidate; they are related to the above-mentioned molecules (dominant D-amino acidate) by a symmetry center.

The packing modes of the present systems are different from those in $[Co(leu)(NH_3)_4]X_2 \cdot H_2O$ (X=Br and I).[2] Two crystal analyses, X=Br with D : L(%)=22 : 78 and X=I with D : L=29 : 71, were performed. They are isomorphous, and all sites in the unit cell have the same

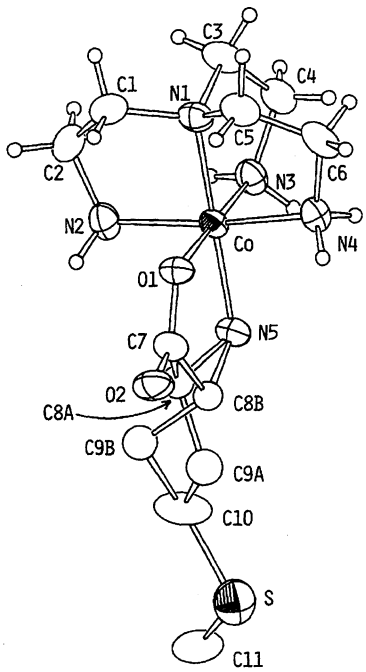

Fig. 6. An ORTEP drawing of *trans*(*N*,*t*-*N*)-[Co(DL-met)(tren)]$^{2+}$ (**3**) with 50% probability level.

Table 7. Selected Torsion Angles (deg)

	1	3
Co–O(1)–C(7)–C(8A)	12.5(6)	−12.5(6)
Co–O(1)–C(7)–C(8B)	−8(1)	11(1)
O(1)–C(7)–C(8A)–N(5)	−31.7(7)	33.3(6)
O(1)–C(7)–C(8B)–N(5)	4(2)	−7(1)
Co–N(5)–C(8A)–C(7)	35.0(5)	−37.0(5)
Co–N(5)–C(8B)–C(7)	2(2)	1(1)
O(1)–Co–N(5)–C(8A)	−24.5(4)	25.6(4)
O(1)–Co–N(5)–C(8B)	−5(1)	3.4(9)
N(5)–Co–O(1)–C(7)	7.5(4)	−7.9(4)
N(1)–C(1)–C(2)–N(2)	−44.2(6)	46.9(6)
N(1)–C(3)–C(4)–N(3)	−37.9(6)	37.4(6)
N(1)–C(5)–C(6)–N(4)	46.1(6)	−44.2(6)
O(1)–C(7)–C(8A)–C(9A)	−154.1(5)	156.1(5)
O(1)–C(7)–C(8B)–C(9B)	139(3)	−127(1)
Co–N(5)–C(8A)–C(9A)	157.9(4)	−160.1(5)
Co–N(5)–C(8B)–C(9B)	−132(3)	110(2)
C(7)–C(8A)–C(9A)–C(10)	−173.3(6)	160.8(5)
C(7)–C(8B)–C(9B)–C(10)	165(2)	−169(1)
N(5)–C(8A)–C(9A)–C(10)	67.5(7)	−78.7(7)
N(5)–C(8B)–C(9B)–C(10)	−64(4)	80(2)
C(8A)–C(9A)–C(10)–C(11)	172.3(7)	—
C(8B)–C(9B)–C(10)–C(11)	−116(3)	—
C(8A)–C(9A)–C(10)–S	—	170.0(5)
C(8B)–C(9B)–C(10)–S	—	83(2)
C(9A)–C(10)–C(11)–C(12)	76(1)	—
C(9B)–C(10)–C(11)–C(12)	108(2)	—
C(9A)–C(10)–S–C(11)	—	174.2(5)
C(9B)–C(10)–S–C(11)	—	144(1)

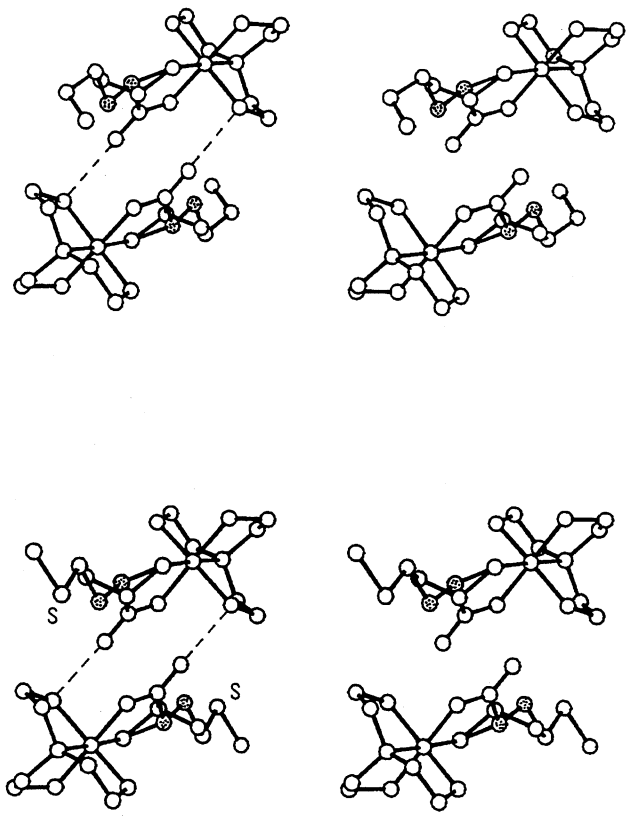

Fig. 7. Stereoviews of the contact pairs in complexes **1** (upper) and **3** (lower). The below complex ions in **1** and **3** are L-rich ones and the dotted circles are major A-atoms. The broken lines show the hydrogen bonds between N(4) and O(2).

composition as its total composition. No deviation of the composition was observed among the sites in the unit cell. This fact means that in a complex with a racemic composition all sites of the unit cell comprise 50% of the D- and 50% of the L-amino acidato complex ions. This seems to be a quite common feature for an ideal, or a pseudo-ideal, solid solution. On the other hand, in the present complexes **1** and **3** with the racemic composition, each site is either D-rich or L-rich. Since there are four sites in the unit cell in both crystals, the two sites are D-rich and the other two sites are L-rich. The total occupancies of the D- and L-molecules in the unit cell are, of course, equal. These are the first examples of the unequal occupancy in each site of the unit cell, with the racemic composition confirmed by an X-ray crystal analysis.

When the crystal composition is changed from the racemic composition to the optically active one in the present system, the symmetric center is lost and becomes a pseudo-symmetric one. However, the solid compositions in the present systems are continuously changeable with the liquid compositions, as shown in the ternary isotherms of Figs. 3 and 4, and all solids are considered to be isomorphous. Therefore, the fundamental aspects of the packing mode are maintained in the optically active compositions. In an optically pure L-crystal the L-molecule has to occupy both sites completely, which were an L-rich site and a D-rich site in the crystal with the racemic composition. This situation is unfavorable from the point of view of free-energy, which is the structural reason why the solubility of the enantiomer becomes higher than that of the racemate.

Layer Structure. There are layer structures in both crystals. Figure 8 shows the intralayer contacts using the ADC code.[5] The repetition of the four

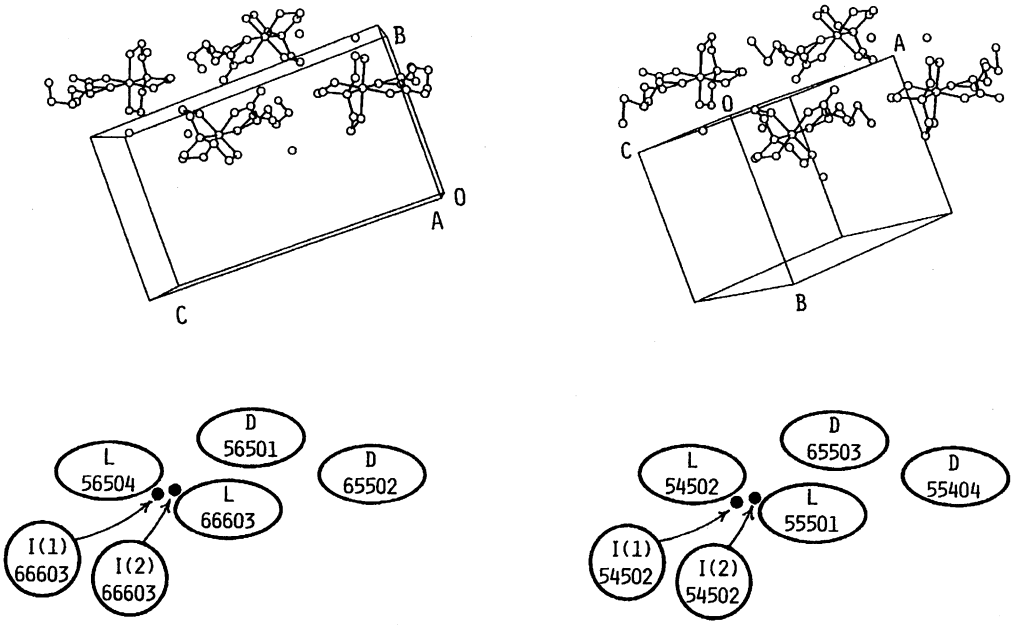

Fig. 8. Comparison of parts of packing of complexes **1** (left) and **3** (right). The below sketches are the absolute configurations of amino acidates with major occupancies and their ADC (atom designator code)[5] notations.

Table 8. Interatomic Distances (Å)

From(ADC)[a)]	To(ADC)[a)]	**1**	**3**
Co(66603)	Co(56501)	7.155(2)	—
Co(66603)	Co(65502)	9.799(1)	—
Co(66603)	Co(56504)	7.883(1)	—
Co(66603)	I(1)(66603)	5.900(1)	—
Co(66603)	I(2)(66603)	4.420(2)	—
I(1)(66603)	N(5)(56504)	3.522(5)	—
I(1)(66603)	Co(65602)	5.091(1)	—
I(1)(66603)	I(2)(66603)	4.771(2)	—
I(2)(66603)	Co(56504)	5.201(1)	—
Co(66603)	Co(76603)	9.204(4)	—
Co(55501)	Co(65503)	—	7.085(2)
Co(55501)	Co(55404)	—	9.630(2)
Co(55501)	Co(54502)	—	7.914(2)
Co(55501)	I(1)(54502)	—	5.782(1)
Co(55501)	I(2)(54502)	—	4.371(1)
I(1)(54502)	N(5)(54502)	—	3.528(5)
I(1)(54502)	Co(56404)	—	5.166(1)
I(1)(54502)	I(2)(54502)	—	4.738(1)
I(2)(54502)	Co(54502)	—	5.290(2)
Co(55501)	Co(45404)	—	9.203(2)

a) Atom designator code:[5)] 1) $(+x, +y, +z)$, 2) $(-x, 1/2+y, 1/2-z)$, 3) $(-x, -y, -z)$, and 4) $(+x, 1/2-y, 1/2+z)$ for **1** and 1) $(+x, +y, +z)$, 2) $(1/2-x, 1/2+y, 1/2-z)$, 3) $(-x, -y, -z)$, and 4) $(1/2+x, 1/2-y, 1/2+z)$ for **3**.

molecules forms a layer. For example, for complex **1** the interatomic Co–Co distances, Co(66603)–Co(56501), Co(66603)–Co(65502), and Co(66603)–Co(56504), are 7.155(2), 9.799(1), and 7.883(1) Å, respectively. The corresponding distances are 7.085(2), 9.630(2), and 7.914(2) Å for complex **3**. Both complexes have very similar values to each other; a full list is given in Table 8. Since the space groups in complexes **1** ($P2_1/c$) and **3** ($P2_1/n$) are merely variant settings of the same one, analogous structures are locally observed.

Complex **1** has accumulated layer structures according to the x-axis, which form the layers (100). Since one layer completely overlaps the next layer in complex **1**, another D-rich complex ion is positioned above a D-rich complex ion. However, there is a slight difference concerning the interlayer relation in complex **3**. Since the next layer shifts to $(\boldsymbol{c}-\boldsymbol{a})/2$, complex **3** has the packing structure of the layers (101): an L-rich complex ion is above a D-rich complex ion and a D-rich complex ion is above an L-rich one. The interlayer distance is 9.204 Å (length of a axis) in complex **1** and 9.177 Å [length of $(\boldsymbol{a}+\boldsymbol{c})/2$] in complex **3**. There is no special short contact between the two layers in either complex.

Supplementary Material Available: Full crystal data, H-atom coordinates, thermal parameters, F_o-F_c tables, and remaining bond lengths and angles.

References

1) J. Jacques, A. Collet, and S. H. Wilen, "Enantiomers, Racemates and Resolutions," Wiley, New York (1981).

2) A. Fuyuhiro, K. Hibino, and K. Yamanari, *Chem. Lett.*, **1991**, 1041.

3) K. Yamanari and A. Fuyuhiro, *Chem. Lett.*, **1991**, 1551.

4) K. Akamatsu, T. Komorita, and Y. Shimura, *Bull. Chem. Soc. Jpn.*, **54**, 3000 (1981).

5) "TEXRAY Structure Analysis Package," Molecular Structure Corporation, 1985.

6) Y. Mitsui, J. Watanabe, Y. Harada, T. Sakamaki, Y. Iitaka, Y. Kushi, and E. Kimura, *J. Chem. Soc., Dalton Trans.*, **1976**, 2095.

7) K. Yamanari, J. Hidaka, and Y. Shimura, *Bull. Chem. Soc. Jpn.*, **46**, 3724 (1973).

8) C. K. Johnson, "ORTEP II. Report ORNL-5138," Oak Ridge National Laboratory, Oak Ridge, TN (1976).